Peculiarities in the interference pattern obtained by x-ray bilens interferometer

Zverev, D. A., Kohn, V. G., Yunkin, V. A., Kuznetsov, S. M., Snigireva, I. I. , et al.

D. A. Zverev, V. G. Kohn, V. A. Yunkin, S. M. Kuznetsov, I. I. Snigireva, A. A. Snigirev, "Peculiarities in the interference pattern obtained by x-ray bilens interferometer," Proc. SPIE 11493, Advances in Computational Methods for X-Ray Optics V, 114930L (21 August 2020); doi: 10.1117/12.2568687

SPIE.

Event: SPIE Optical Engineering + Applications, 2020, Online Only

Peculiarities in the interference pattern obtained with X-ray bilens interferometer

D. A. Zverev[a], V. G. Kohn[b], V. A. Yunkin[c], S. M. Kuznetsov[c], I. I. Snigireva[d], and A. A. Snigirev[a]

[a]Immanuel Kant Baltic Federal University, Gaidara 6, Kaliningrad 236041, Russian Federation
[b]NRC "Kurchatov Institute", Kurchatov square, 1, Moscow 123182, Russian Federation
[c]Institute of Microelectronics Technology RAS, Chernogolovka 142432, Russian Federation
[d]European Synchrotron Radiation Facility, 71 Avenue des Martyrs, Grenoble 38043, France

ABSTRACT

We present a study of optical properties of the bilens interferometer, where there is a space (Si bulk volume) between two compound refractive lenses (CRL). This design was proposed by analogy with the well-known Billiet bilens for the visible light. It was experimentally shown that under the conditions of partial absorption of X-ray radiation by the bilens, the generated interference pattern has a double period for several central fringes instead of pattern with a constant period. It was shown by computer simulation of such peculiar interference patterns that this phenomena is due to the additional interference between the rays focused by bilens and rays transmitted through the Si material between lenses in bilens. This fact encourages us to propose a new design for bilens and multilens interferometers, in which there is no spacing between CRLs. The proposed design is the lens arrays in the interferometer are arranged in a chessboard pattern, i. e. the arrays are shifted relative to each other by the distance equal to half-length of the single lens.

Keywords: X-ray focusing, compound refractive lens, X-ray interference, bilens interferometer, X-ray absorption

1. INTRODUCTION

Nowadays, the continuous evolution of synchrotron radiation sources has resulted in a dramatic increase of brilliance and degree of spatial coherence with respect to older designs. The availability of such intense coherent X-ray beams has triggered the development of wave splitting interferometers similar to the classical double-slit Youngs experiment[1] where interference of two coherent beams created by two narrow slits occurs. Another way to produce a coherent narrow beam is to use X-ray refractive optics elements, namely, compound refractive lenses (CRL).

X-ray refractive optics has been developed soon after an advent of the first synchrotron radiation source of third generation in Grenoble (France).[2] First lenses were very simple. They consisted of a set of holes in the block of aluminium or berillium, i.e. materials with a high ratio refraction/absorption, which allow easy mechanical process. For the years from 1996 till now large success was achieved in developing various more advanced technologies of creation of compound refractive lenses (CRL). See the review[3–5] for more details.

The CRLs with a parabolic profile of refracting surface are the most interesting, and, among them, the planar lenses which can be constructed with a very accurate parabolic profile of very small curvature radius. Today the lenses of such a type allows one to focus an x-ray beam to a size of hundred nanometers, and there is a possibility of beam compress to smaller sizes in the focus.[6]

The planar lenses are manufactured in the monocrystal silicon wafer by using a microfabrication process involving electron beam lithography and anisotropic deep plasma etching The ability of technology to create the

Further author information: (Send correspondence to D. A. Z.)
D. A. Z.: E-mail: daswazed@yandex.ru,
I. I. S.: E-mail: snigireva@esrf.fr,

Advances in Computational Methods for X-Ray Optics V, edited by Oleg Chubar, Kawal Sawhney, Proc. of SPIE Vol. 11493, 114930L · © 2020 SPIE
CCC code: 0277-786X/20/$21 · doi: 10.1117/12.2568687

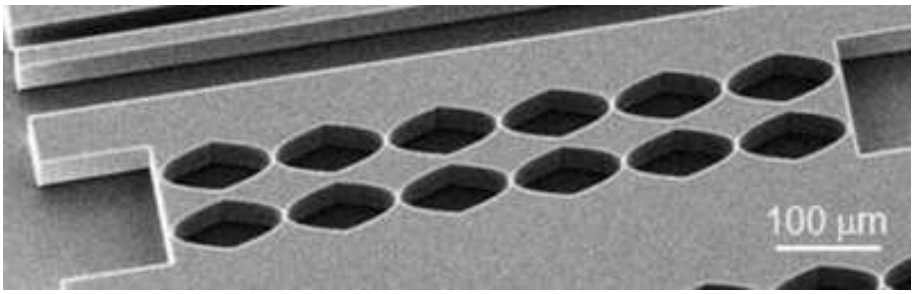

Figure 1. Image of the interferometer with 6 double concave elements obtained with a scanning electron microscope

CRLs with very small curvature radius, and, as a consequence, with a relatively small aperture, allows one to make a next step. Namely, the x-ray bilens interferometer was created on the base of two CRLs placed closely one to another.[7] This interferometer is similar to well-known Billiet bilens for the visible light.

Two CRLs compress the wave from the real source with creating two focuses which can be considered as secondary sources of coherent divergent radiation. The divergence of the waves from such secondary sources is determined by angular aperture of the CRLs, i.e. by the ratio of the effective CRL aperture[8] and the focus distance. Nevertheless, the waves which go from these two sources overlep each other at some distance with creation of interference fringes as a periodic change of intensity in space.

A period of such structure is linearly proportional to a distance from the sources. Consequently, one can place a detector on various distances from the interferometer and observe the x-ray standing wave with various period from tens of nanometers to tens of micrometers. Just this device allows one to demonstrate experimentally a possibility of creation of x-ray standing wave with the period less than micron[9]

New device was called x-ray nanointerferometer. Since direct methods of detecting space distribution of x-ray intensity with nanometer period are absent, authors used a test sample as a periodic Ta lattice with the period of 400 nm. Both the moire fringes for small difference between periods of Ta lattice and x-ray standing wave, and a periodic change of integral intensity during a small displacement of the Ta lattice across the beam were observed.

The x-ray interferometer has some specific features. Particularly, any CRL both refracts and absorbs the x-ray beam simultaneously. The absorption leads to the fact that only the central part of small matter thickness can focus the beam. As a result, the effective aperture of CRL is always smaller than the geometrical aperture. This leads to a consequence that the overlap of beams from different focuses occurs at longer distances.

On the other hand, the first design of the interferometer includes Si bulk volume between the CRLs with the longitudinal thickness which is equal to a total thickness of CRL. This design was proposed to the analogue of the well-known Billiet bilens for the visible light where two half- lenses are separated by the air gap. A detailed experimental investigation shows that this bulk volume yields in peculiarities in the interference pattern obtained with X-ray bilens interferometer if that volume does not absorb the beam completely. The part of the beam which propagates through the bulk volume disturbs the interference fringes in the central part. As a result, the interference picture contains four or five fringes with a double period depending on the distance between the interferometer and the detector.

In this paper we present experimental results and computer simulation of interference pattern with non-constant periodicity. The computer simulation of the interference fringes for this model of interferometer allows

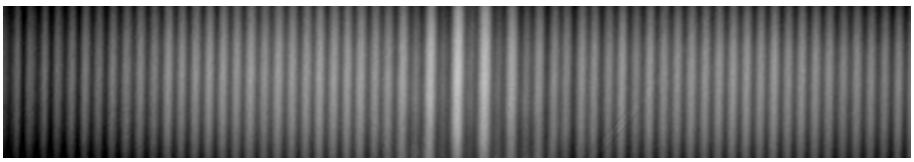

Figure 2. A central fragment of interference fringes ontained with BI6 interferometer rotated on 90 degree

us to study the effect in details, i.e. to observe periodic disturbance of the stangard fringes with appearance consequently four or five or zero fringes of double period depending on the distance. To eliminate this undesirable effect we elaborate a new design of the interferometer where the CRL are close one to another transversally and are shifted on the half length of one single element of CRL.

2. EXPERIMENTAL RESULTS

The first design of x-ray bilens interferometer consists of two CRLs with a spacing between them. CRLs consists of single lenses with the geometric aperture $A = 50$ μm and the curvature radius near the apex of parabola $R_0 = 6.25$ μm. The spacing between the CRLs is $d_0 = 10$ μm. The silicon chip (a piece of the Si wafer) contains 5 bilens interferometers with various number of single lenses – 6, 26, 58, 104 and 162. Each single lens has web of thickness 2 μm, where the web is a distance between two parabolic refracting surfaces at the apex. These webs lead to additional absorption of the radiation wave without disturbance of its space structure.

The experiments were performed with the synchrotron radiation source of third generation ESRF in Grenoble (France). The more pronounced phenomena of non-constant period took place for some relations between the number of elements in CRL and the energy of x-ray photons. Namely, it was required that the decrease in intensity due to absorption in the bulk volume was comparable to the decrease in intensity due to angular divergence of radiation after focusing. This was the condition for the best interference of rays traveling to the same point along different paths.

In this section we present the result of measuring the interference fringes from the bilens interferometer (BI6) consisting of 6 double concave elements. Figure 1 shows the image of this interferometer obtained with a scanning electron microscope. Figure 2 shows a central fragment of interference picture observed at the following conditions: energy 12 keV (wave length $\lambda = 0.1033$ nm), distance from the source to the BI6 $z_0 = 54$ m, distance from the BI6 to the detector $z_1 = 5.3$ m, the effective source size $S = 50$ μm, exposition time 5 sec.

The source has minimum size, pointed above, in a vertical plane. Correspondingly, the interference picture was detected in the vertical plane too. Figure 2 shows a picture rotated on 90 degree for a convenience. It is easy to see on the figure 2 that the interference fringes far from the centre has a right periodic structure with the period 8.9 μm that is well correspondent to the theory. The theoretic estimation on the period Λ can be calculated by formula

$$\Lambda = \frac{\lambda(z_1 - z_f)}{d_1(1 + z_f\,/z_0)} = \frac{\lambda}{d_1}\left(z_1 - f\,\frac{z_t}{z_0}\right) \tag{1}$$

where $d_1 = 60$ μm is a distance between two focuses,

$$z_t = z_0 + z_1, \quad z_f = \frac{f}{1 - f\,/z_0} \tag{2}$$

This formula just gives $\Lambda = 8.9$ μm for the values pointed above and $f = 15.4$ cm.

However, the central part of interference picture has another structure. It consists of four fringes with high contrast and a double period, and thin fringes of weak contrast between them. This structure is not universal. For various distances z_1 the number of high contrast fringes may be four, five or zero. We observed as well that a replacement of BI6 by interferometer with larger number of elements leads to disappearing the artefact, but it can appear again for larger energy of x-ray photons.

3. COMPUTER SIMULATION

Computer simulations of optical properties of bilens interferometer was performed with the program written on the programming language ACL[10] with the language interpreter written in Java. The calculations are similar to simulations of x-ray phase contrast from microobjects.[11] It is assumed that a spherical monochromatic wave from the point source illuminates the object, particularly, a bilens. The Bilens has a small thichness as compared to a focal distance. Then change of X rays trajectories inside the bilens can be neglected, and transmission of wave through bilens can be accounted for through a complex phase shift

$$\varphi(x) = k\,[-\delta + i\beta]\,t(x) \tag{3}$$

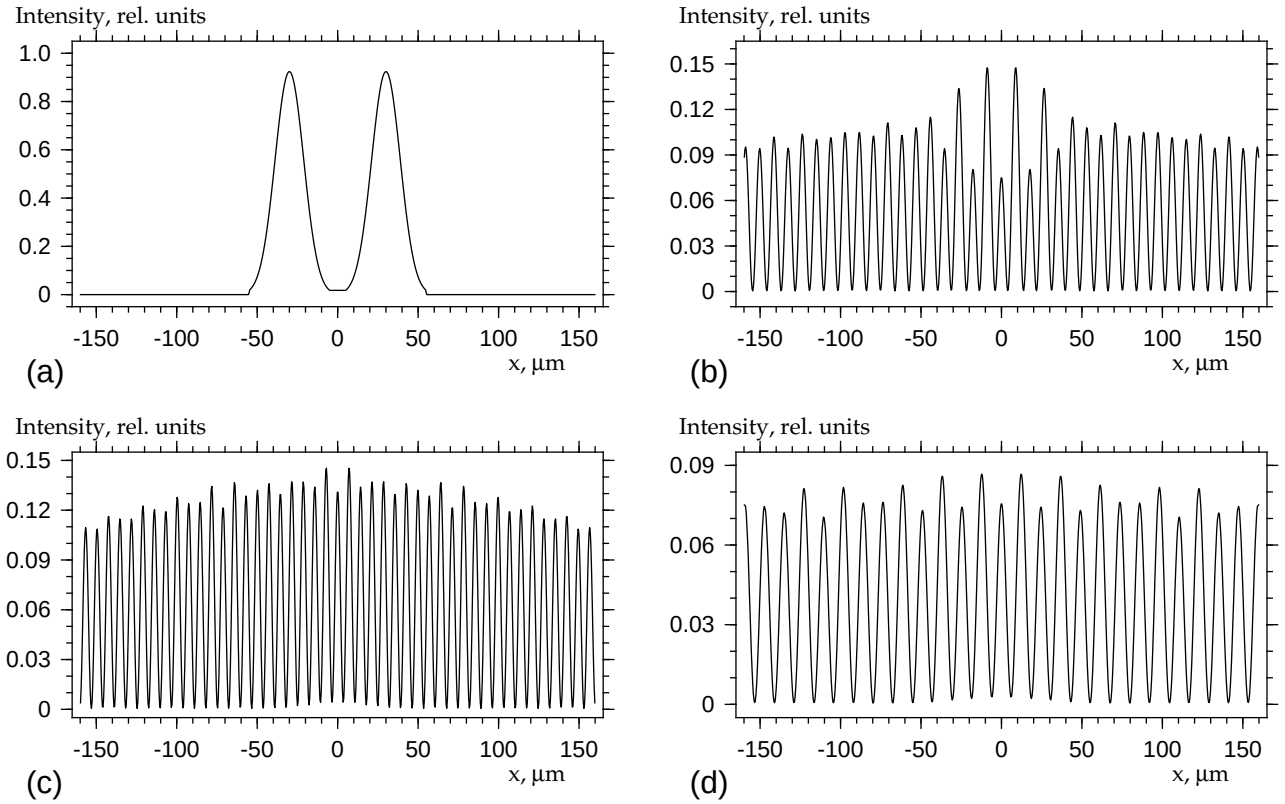

Figure 3. Computer simulations of interference fringes: (a) BI6, distance 0 cm; (b) BI6, distance 530 cm (c) BI6, distance 430 cm; (d) BI6, distance 730 cm;

where $k = 2\pi/\lambda$ is a wave number, the complex refractive index of material $n = 1 - \delta + i\beta$, and $t(x)$ is a thickness of material inside the object along the ray having a transverse coordinate x.

We are not interested in a specific distribution of material inside the CRL. The CRL may have N double concave elements with the curvature radius $R_0 = RN$ or may have only one element with the curvature radius R. In our approximation all such configurations are equavalent. Practically, a usage of CRL allows one to obtain the effectve lenses with very small curvature radius, that is necessary for decreasing the focal distance which in our approximation is determined as $f = R/2\delta$.

In the theory it is simpler to deal with the lens consisting from one element, that we will assume below. For the x-ray bilens interferometer $t(x)$ is determined as follows

$$\begin{array}{ll} t(x) = (x - x_k)^2/R, & |x - x_k| < A/2 \\ t(x) = t_0, & |x| < d_0/2 \\ t(x) = t_1, & |x| < d_0/2 + A \end{array} \tag{4}$$

Here $x_k = \pm(A + d_0)/2$, $k = 1, 2$, $t_0 = A^2/4R$, t_1 – thickness of matter outside the interferometer (see figure 1). As a rule t_1 is so much that the radiation is absorbed fully.

Let $E_0(x)$ be a wave function of radiation in front of interferometer, and we are interested by a distibution along the coordinate x. The transmission of radiation through the interferometer is described by a simple multiplication on the exponential which takes into account the phase shift

$$E_1(x) = E_0(x) \exp(i\varphi(x)). \tag{5}$$

Subsequent propagation of wave function in free space is calculated as a convolution of $E_1(x)$ with the Fresnel

Figure 4. Design of bilens interferometers with a space between two CRLs: (a) spacing 10 μm, (b) zero spacing and (c) zero spacing and shift.

propagator

$$P(x) = (i\lambda z_1)^{-1/2} \exp\left(i\pi \frac{x^2}{\lambda z_1}\right) \tag{6}$$

where a distance z_1 is determined above as a distance between the interferometer and the detector.

The convolution is calculated by means of Fourier transformation. First, a Fourier image of $E_1(x)$ is calculated numerically. Then it is multiplied by the Fourier image of Fresnel propagator which is known analytically. Finally, the reverse Fourier image of a product, calculated numerically, gives the wave function in front of the detector. The intensity is a square modulus of the wave function. To take into account the source size, the intensity is convoluted with the Gaussian having FWHM (full width at half maximum) $s = S(z_1/z_0)$ where S is a tansverse source size.

The program allows one to calculate the intensity distribution for any distance, radiation wave length and any parameters of inteferometer under the condition that a thickness of the interferometer is several times smaller

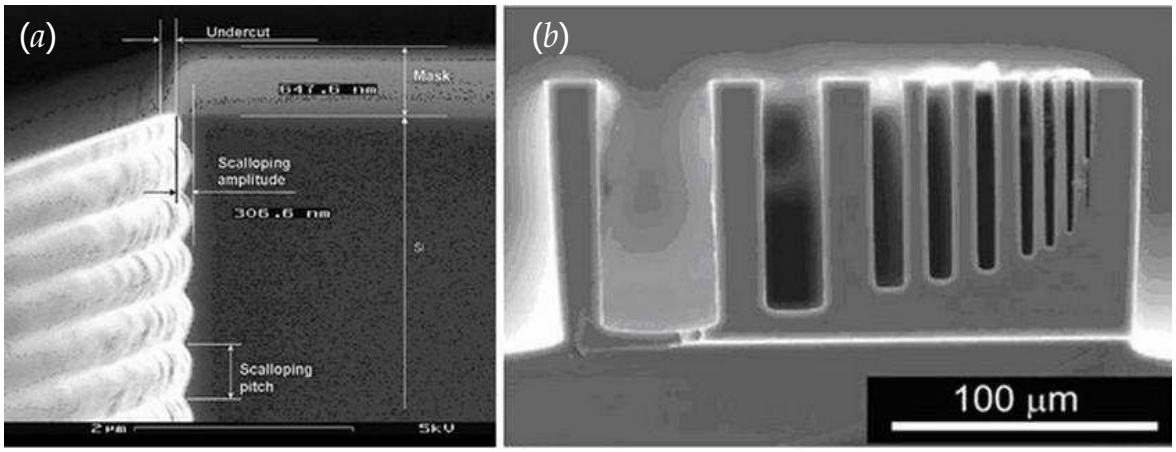

Figure 5. SEM cross-sectional images of silicon (a) refractive lens and (b) test structure with trenches of different width[13]

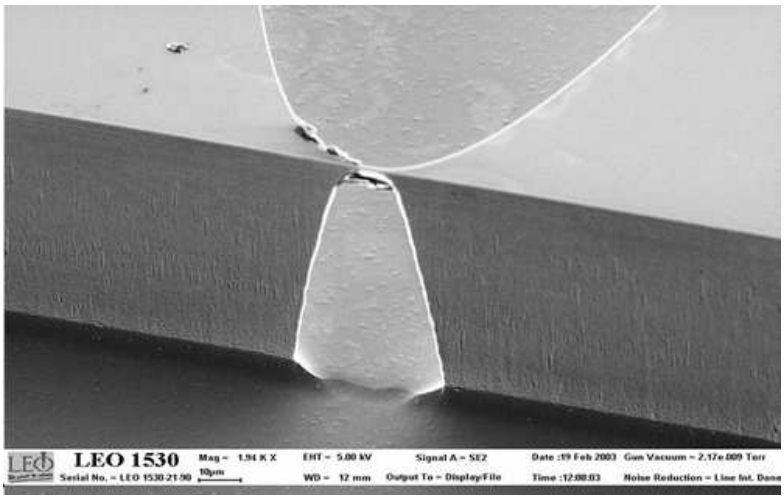

Figure 6. SEM image of Si parabolic lens with distorted refractive surface

the focal length. Figure 3 shows the results of calculation for the BI6 and the photon energy 12 keV. In this case the interferometer thickness $t_0 = 0.612$ mm is not large, and the wave function modulus is decreased by the factor 0.27 due to absorption. The calculations were performed for the experimental conditions pointed in preceding section but the distance z_1 was variable.

The figure 3a shows the profile of relative intensity just behind the interferometer for the distance $z_1 = 0$. It is seen that the intensity in the region between the lenses is very small, but it is not the case for the wave amplitude wich take part in the interference. The fogure 3b shows the central part of interference picture for the distance $z_1 = 530$ cm. The period of interference fringes at the left ans at the right is correspondent to the theory for the ideal bilens, and the distribution is close the the sine function. However, the fringes of central part are different. It is evident that here we see extra-interference between the rays from the bilens focuses and rays propagated through the plane parallel fragment of the bilens. Particularly, this interference becomes destructive for the central peak at $x = 0$.

As it is shown from computer simulations this peculiarity depends on the distance z_1. With decreasing the distance z_1 this peculiarity becomes less pronounced, and, finally, at the distance $z_1 = 430$ cm it disappears at all. The intensity profile for this distance is shown in figure 3c. Some small difference between the peaks takes place but the period of fringes is constant. Further decreasing the distance z_1 leads to appearence exta-interference again, and it is best pronounced at the distance $z_1 = 350$ cm. But this time the central peak is well pronouced and number of central peaks of double period is five.

With decreasing the distance z_1 further the extra-interference disappears again at the distance $z_1 = 290$ cm. We note that the interval of distances for which the extra-interference disappears is very short while the interval of well pronouced extra-interference is rather long. The described picture repeats itself again and again with decreasing z_1, and changes are observed faster. So for $z_1 = 250$ cm the interference picture is practically the same as shown in figure 3b, but with smaller period correspondingly the distance.

With increasing the distance z_1 the extra-interference disappears at the distance $z_1 = 730$ cm. This case is shown in figure 3d. For large distances change of interference structure occurs with decreasing speed. Thus, the results of computer simulations coincide completely with the experimental data. Detailed analytical analysis of this extra-interference is out of the scope of our work. Our aim is to demonstrate an interesting phenomena of complex interference which is possible for the bilens interferometer of such a type, as well as to show a possibilty of the program to investigate peculiarities of intereference picture for such interferometer.

The ways of elimination of this extra-interference is discussed in the next section. The calculations show that the bilens interferometer without the plane parallel fragment gives the pure interference fringes in the central part for all distances where the interference takes place for the rays far from the aperture edges. However, for small distances the aperture edges can distort the picture.

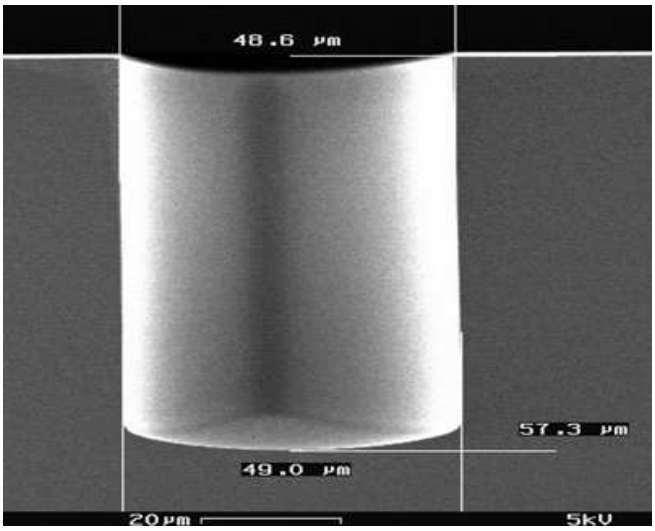

Figure 7. SEM cross-sectional image of silicon parabolic lens with nearly vertical sidewalls[13]

Bilens interferometer BI26 with 26 double concave elements has a thickness $t_0 = 2.6$ mm and the focal distance $f = 3.55$ cm for energy 12 keV. In this case decreasing the wave function modulus is by the factor 0.003, and the plane parallel fragment does not destroy the periodicity of the fringes. But the same phenomena will appear for the higher energies. It is of interest how small period can be obtained with BI26. The focal distance for this device is smaller but the effective aperture is smaller as well. The simulations show that apparent standing wave can be observed at $z_1 = 14$ cm with the period 180 nm and relatively small contrast.

We note finally that the computer program is a very useful tool for study of optical properties of bilens interferometer which allows us both to explain the observed experimental data and to forecast new ones.

4. NEW DESIGN OF BILENS INTERFEROMETER

As it was shown above the Si bulk volume between two CRLs in bilens interferometer (figure 1) is an issue for generation the pure standing wave with a constant period. The simplest solution is to reduce this bulk volume (i.e. make zero spacing between the CRLs) without any additional changes in the CRLs design (figure 4b).

However, manufacturing of the bilens interferometer with zero spacing is a technological issue due to some features of deep silicon plasma etching in Bosch process[12] applied for silicon planar refractive lenses[13] and the bilens interferometer[6] fabrication. It was shown[14] that conventional Bosch processing leads to mask undercut and lens sidewall roughness (scalloping) (Fig. 5a) originated from cyclic plasma isotropic etching and polymer film deposition.

In addition Bosch process is accompanied by the aspect ratio dependent etching (ARDE) effect when etching trenches with different width.[13] As shown in figure 5b etched depth, shape and sidewall slope of trenches depend on the trench width.

The mask undercut, sidewall roughness and ARDE effect may lead to the lens shape errors and to deviation of refractive surface of parabolic lens from the ideal one. It has been shown[13] that mask undercut and negatively sloped sidewall etching resulted in large deviations and discontinuity of the lens refractive surface (Fig. 6) that had strong negative effect on lens performance.

In turn, the sidewall roughness caused by scalloping results in worsening of the interference pattern contrast. Special efforts were spent on improving the fabrication accuracy of the refractive lenses. To control sidewall verticality of the etched parabolic lenses we modified parameters of conventional Bosch process (Fig. 7).

To control parabolic lenses critical dimensions related to the mask undercutting during the etching process special bias in lens design was developed and applied. This special bias has compensated a shift of parabolic lens boundaries, caused by the mask undercut.

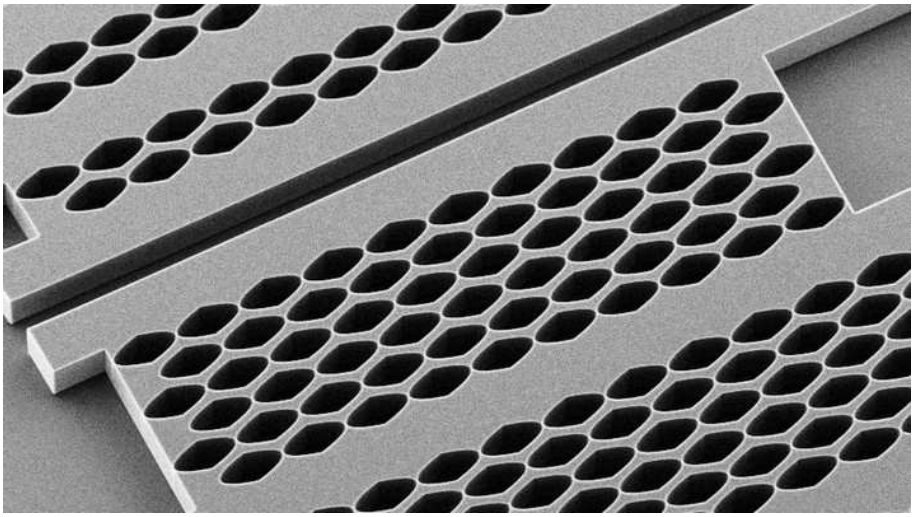

Figure 8. SEM image of silicon bilens and sixlens interferometers of new design

The scalloping amplitude of lens refractive surfaces was decreased by optimization of etching and passivation steps duration or cycle time in a modified Bosch process. In addition, silicon chip with etched lenses was first thermally oxidized and then silicon oxide was removed by wet etching.

The proposed approaches and optimized processes made it possible to control the fabrication accuracy, reducing the lens shape errors. Silicon parabolic lenses with nearly vertical and smooth (with ¡ 25 nm scalloping amplitude) sidewalls were fabricated for high energy X-ray nanofocusing.[14] However, the available technology allowed one to control the mask undercut with accuracy of about 100 nm. This fabrication parameters didnt allow us to manufacture bilens interferometer with zero spacing between CRLs shown in figure 4b. Therefore we proposed new design of the interferometer (Fig. 4c) with zero spacing.

In the new design one CRL was shifted on half length of a single lens parallel to the second CRL so that CRLs are arranged in a chessboard pattern; i.e. the lens arrays are shifted relative to each other by the distance equal to half-length of the single lens. This design also allows to reduce the transversal size of the interferometer. This approach was accepted as basic for development and fabrication of interferometers bases on two or more CRLs (Fig. 8).[15,16]

ACKNOWLEDGMENTS

This work was supported by the Russian Foundation for Basic Research (project 19-29-12043mk). VAY and SMK were partly supported by the State Task No. 075-00920-20-00.

REFERENCES

[1] W. Leitenberger, S. Kuznetsov, A. Snigirev, "Interferometric measurements with hard X-rays using a double slit", Optics Communications, 191, 91-96 (2001)

[2] A. Snigirev, V. Kohn, I. Snigireva, B. Lengeler, "A compound refractive lens for focusing high-energy X-rays", Nature, 384, 49-51 (1996).

[3] I. Snigireva, A. Snigirev, X-ray microanalytical techniques based on synchrotron radiation, J. Environ. Monit., 8, 33 42 (2006).

[4] A. Snigirev, I. Snigireva, High energy X-ray microoptics, C. R. Physique, 9, 507-516 (2008).

[5] S. Bajt, C. G. Schroer, "Sub-micrometer Focusing and High-Resolution Imaging with Refractive Lenses and Multilayer Laue Optics", in the book: "Synchrotron Light Sources and Free-Electron Lasers", pp 1161-1188 (2020).

[6] A. Snigirev, I. Snigireva, M. Grigoriev, V. Yunkin, V. Di Michiel, G. Vaughan, V. Kohn, S. Kuznetsov, "High energy X-ray nanofocusing by silicon planar lenses", J. Phys.: Conf. Series 186, 012072 (2009).
[7] A. Snigirev, V. Kohn, I. Snigireva, M. Grigoriev, S. Kuznetsov, V. Yunkin, T. Roth, C. Detlefs, G. Vaughan, "Hard X-ray interferometer based on a silicon refractive bi-lens system", ESRF Highlights 2008, Eds. G. Admans, 125-126 (2009).
[8] V. G. Kohn, "Effective aperture of X-ray compound refractive lenses", J. Synchrotron Rad., 24, 609-614 (2017).
[9] A. Snigirev, I. Snigireva, V. Kohn, V. Yunkin, S. Kuznetsov, M. Grigoriev, T. Roth, G. Vaughan, C. Detlefs, "X-Ray Nanointerferometer Based on Si Refractive Bilenses", Phys. Rev. Lett., 103, 064801 (2009)
[10] V. G. Kohn, web site: http://kohnvict.ucoz.ru/vkacl/vkACLde.htm
[11] A. Snigirev, I. Snigireva, V. Kohn, S. Kuznetsov, I. Schelokov, "On the possibilities of x-ray phase contrast microimaging by coherent high-energy synchrotron radiation", Rev. Sci. Instrum. 66, 5486-5492 (1995).
[12] F. Laermer, A. Schilp, "Method of anisotropically etching silicon" U.S. Patent No. 5501893 (1996)
[13] V. Yunkin, M. Grigoriev, S. Kuznetsov, A. Snigirev, I. Snigireva, "Planar parabolic refractive lenses for hard x-rays: technological aspects of fabrication", Proc. SPIE 5539, 226-234 (2004).
[14] A. Snigirev, I. Snigireva, M. Grigoriev, V. Yunkin, M. Di Michiel, S. Kuznetsov, G. Vaughan, "Silicon planar lenses for high energy x-ray nanofocusing", Proc. SPIE 6705, 670506-(1-8) (2007) .
[15] A. Snigirev, I. Snigireva, M. Lyubomirskiy, V. Kohn, V. Yunkin, S. Kuznetsov,"X-ray multilens interferometer based on Si refractive lenses", Optics Express, Vol. 22, 2584225852 (2014).
[16] M. Lyubomirskiy, I. Snigireva, V. Kohn, S. Kuznetsov, V. Yunkin, G. Vaughan, A. Snigirev, "30-lens interferometer for high-energy X-rays", J. of Synchr. Rad., 23, 11041109 (2016)